Journal of Organometallic Chemistry 791 (2015) 303–310

Contents lists available at ScienceDirect

Journal of Organometallic Chemistry

journal homepage: www.elsevier.com/locate/jorganchem

Synthesis and reactivity of (pyrazol-1-yl)acyl iron complexes

Da-Wei Zhao, Yi Xu, Yao-Wei Guo, Hai-Bin Song, Liang-Fu Tang*

Department of Chemistry, State Key Laboratory of Elemento-Organic Chemistry, Collaborative Innovation Center of Chemical Science and Engineering, Nankai University, Tianjin 300071, People's Republic of China

ARTICLE INFO

Article history:
Received 1 April 2015
Received in revised form
4 June 2015
Accepted 6 June 2015
Available online 10 June 2015

Keywords:
Pyrazole
Pyridine
Iron carbonyl
Metal-acyl complex
Thiolate

ABSTRACT

Treatment of 1-methyl-3,5-dialkylpyrazoles with *n*-BuLi, and subsequently with iron carbonyl and iodine yielded (pyrazol-1-yl)acyl iron complexes $CH_2(CO)$ (3,5-R_2Pz)$Fe(CO)_3I$ (R = Me or Pr^i, Pz = pyrazol-1-yl). Reaction of $CH_2(CO)$ (3,5-Me_2Pz)$Fe(CO)_3I$ with PhSNa gave a dimeric complex [$CH_2(CO)$ (3,5-Me_2Pz) $Fe(CO)_2(SPh)]_2$, while similar reactions of $CH_2(CO)$ (3,5-R_2Pz)$Fe(CO)_3I$ with PySNa (Py = 2-pyridyl) gave mononuclear complexes $CH_2(CO)$ (3,5-R_2Pz)$Fe(CO)_2(SPy)$, which exhibited an isomerization in solution. Treatment of the dimeric complex with PPh_3 at room temperature resulted in the decomposition of the starting material. Furthermore, this dimeric complex readily underwent reductive elimination to generate $CH_2(COSPh)$ (3,5-Me_2Pz) when heated at relatively low temperature, and thermal decomposition reaction to give PhSSPh in refluxing toluene solution. Reaction of mononuclear complexes with PPh_3 caused one carbonyl to be replaced by phosphine ligand to give complexes $CH_2(CO)$ (3,5-R_2Pz) $Fe(CO)$ (PPh_3) (SPy). All these acyl iron complexes were fully characterized by IR and NMR spectroscopy, and their structures were unambiguously determined by X-ray crystallography.

1. Introduction

The metal-acyl complexes are of great importance since they have proven to be excellent homogenous catalysts or crucial active intermediates in many important organic transformations [1–5], especially such as catalytic carbonylation reactions [6–9]. Furthermore, the metal-acyl unit has been introduced into the main chain of polymers to form potential functional organometallic materials [10,11], which develops the new application fields of metal-acyl complexes. In addition, since the successful elucidation of the structure of [Fe]-hydrogenase [12] indicated that an acyl-iron ligates to the active site of [Fe]-hydrogenase [13–15], many acyl iron complexes have been synthesized as biomimetic models for the active site of [Fe]-hydrogenase [16–25], which greatly promotes the development of metal-acyl complexes and widely broadens the potential application areas of metal-acyl complexes. Our recent investigations showed that polydentate pyrazolyl-based ligands could potentially be used to stabilize metal-acyl complexes [26–28]. These interesting results encouraged us to explore other related metal-acyl complexes based on pyrazolyl-based ligands. On the other hand, it is known that the chelation-assisted effect of polydentate ligands not only plays an important role in stabilizing metal-acyl complexes during their formation [29–31], but also significantly affects their reactivity [3]. As a part of our investigations on the metal-acyl complexes, in order to deeply understand the effect of the chelation-assisting roles of polydentate ligands on the reactivity and properties of the corresponding metal-acyl complexes, in this paper we describe the synthesis and reactivity of new pyrazolyl-based iron complexes containing bidentate (pyrazol-1-yl)acyl ligands.

2. Results and discussion

2.1. Synthesis of (pyrazol-1-yl)acyl iron complexes

It is known that *N*-alkyl-3,5-dialkylpyrazoles underwent lithiation exclusively at the α-position of the *N*-alkyl groups [32], and the resulting lithium salts could react with various electrophiles, leading to the corresponding carbanions as important synthetic intermediates. Herein we find that treatment of the 1-lithio derivatives of 1,3,5-trimethylpyrazole and 1-methyl-3,5-diisopropylpyrazole with $Fe(CO)_5$ followed by I_2 yields (pyrazol-1-yl)acyl iron complexes **1** and **2** (Scheme 1). These two complexes were air-stable in the solid state and their solution could be manipulated in air for a short time without notable decomposition. They were fully characterized by IR and NMR spectroscopy.

* Corresponding author.
E-mail address: lftang@nankai.edu.cn (L.-F. Tang).

http://dx.doi.org/10.1016/j.jorganchem.2015.06.008
0022-328X/

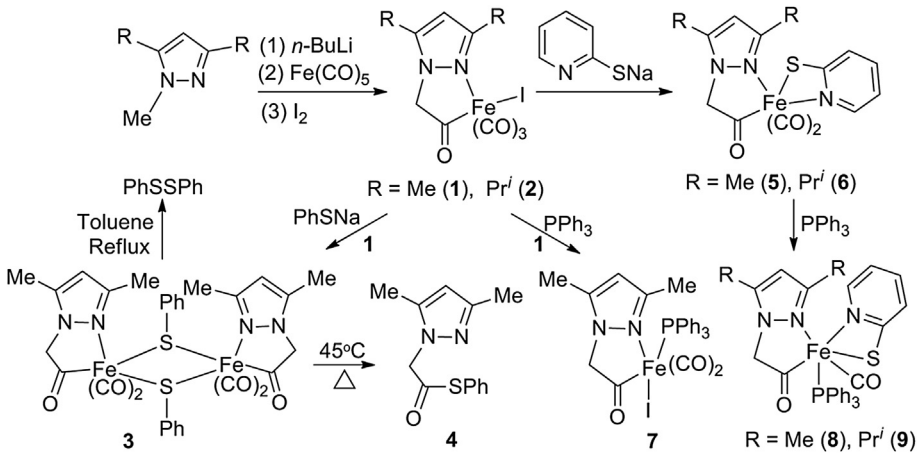

Scheme 1. Synthesis and reactivity of (pyrazol-1-yl)acyl iron complexes.

The IR spectra of **1** and **2** showed that the characteristic acyl carbonyl (C═O) peak occurred at 1667 and 1676 cm^{-1}, respectively, lower than those in tridentate acyl ligated iron complexes, but higher than those in monodentate acyl ligated iron complexes [26]. The corresponding acyl carbons resonated at 254.0 ppm (**1**) and 254.2 ppm (**2**) in their ^{13}C NMR spectra, which were comparable to those in monodentate and tridentate acyl ligated iron complexes [26]. In addition, the protons of the methylene group of these two complexes displayed an AB system in their ^{1}H NMR spectra, indicating that the five-membered metallacyclic structure was reserved in solution, which resulted in these two diastereotopic protons. Furthermore, four sets of proton and carbon signals of the isopropyl methyl groups were observed in the ^{1}H and ^{13}C NMR spectra of **2**, reflecting that their free rotation was hindered possibly due to the repulsion among the bulky isopropyl groups.

2.2. Reaction of (pyrazol-1-yl)acyl iron complexes with ArSNa (Ar = Ph or 2-pyridyl)

Reaction of **1** with PhSNa gave a dimeric complex (**3**) (Scheme 1). The oxidative addition of thioesters to iron(0) to afford acyl thiolato iron complexes is known [16,17], but the dimeric complex readily underwent reductive elimination to generate S-phenyl (3,5-dimethylpyrazol-1-yl)thioacetate (**4**) when heated at relatively low temperature (45 °C), and thermal decomposition reaction to give PhSSPh in refluxing toluene solution. Additionally, compound **4** was easily decomposed to afford PhSSPh with other uncharacterizable products when heated in refluxing toluene. Some analogous spectroscopic features were observed in complexes **1**–**3**. For example, their IR spectra showed a resembling acyl carbonyl absorption peak. The ^{1}H NMR spectrum of **3** also displayed the inequivalent methylene protons, similar to those in **1** and **2**. The structure of **3** was further confirmed by X-ray crystallography, and is shown in Fig. 1. The (pyrazol-1-yl)acyl group is bonded to the iron atom in a bidentate κ^2-[N,C] chelating fashion. The Fe–S bond distances (2.347–2.408 Å) are unequal, but comparable to those reported in other acyl diiron complexes with the μ-SPh group, such as 2.3102–2.3972 Å in $Fe_2(SPh)_2[Ph_2PC_6H_4C(O)]_2(CO)_3$ [16]. The Fe–C_{acyl} and Fe–N bond distances are similar to the corresponding values reported for tridentate chelating bis(pyrazol-1-yl)acyl iron derivatives [26]. The C–C_{acyl} bond distance is 1.544(6) Å, close to those in monodentate acyl iron complexes, but slightly shorter than those in tridentate acyl iron complexes [26].

Reaction of **1** and **2** with PySNa (Py = 2-pyridyl) gave mononuclear complexes **5** and **6**, respectively. The substitution of iodide by 2-pyridinethiolate caused the characteristic acyl carbonyl peaks of **5** (1650 cm^{-1}) and **6** (1655 cm^{-1}) in their IR spectra to significantly shift toward lower wave numbers compared to those of **1** and **2**, which should be attributed to the stronger donor ability of 2-pyridinethiolate than iodide strengthening metal to carbonyl back bonding. The ^{1}H and ^{13}C NMR spectra of **5** and **6** displayed two sets of proton and carbon signals, indicating the presence of isomers (Scheme 2). The assignment of isomers was based on the NOE experiments and the X-ray crystal structure determination of isomer **5A** (Fig. 2). Though the high similarity in the properties of **5A** and **5B** complicated the spectra, two sets of signals with a ratio of *ca.* 4/1 in $CDCl_3$ were clearly integrated for the two isomers respectively. For the signal set with larger integrals, strong correlation was observed in the NOESY spectrum between the methyl signal at 1.68 ppm and the aromatic proton at 8.10 ppm which should be the

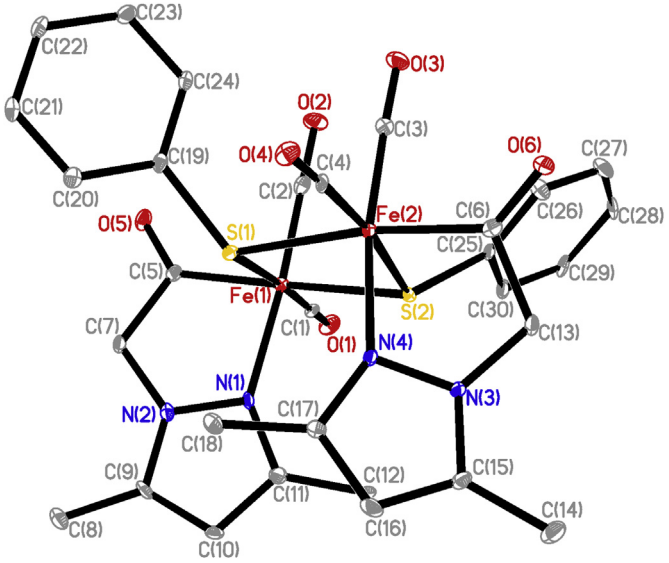

Fig. 1. The molecular structure of **3**. The thermal ellipsoids are drawn at the 30% probability level. Selected bond distances (Å) and angles (°): Fe(1)–S(1) 2.347(2), Fe(1)–S(2) 2.408(1), Fe(1)–N(1) 2.033(4), Fe(1)–C(5) 1.938(5), Fe(2)–S(1) 2.402(1), Fe(2)–S(2) 2.347(2), Fe(2)–N(4) 2.039(3), Fe(2)–C(6) 1.945(5), C(5)–O(5) 1.213(5), C(6)–O(6) 1.217(5), C(5)–C(7) 1.544(6) Å; C(5)–Fe(1)–S(2) 166.6(2), C(5)–Fe(1)–N(1) 84.1(2), C(6)–Fe(2)–S(1) 171.4(2), C(6)–Fe(2)–N(4) 82.1(2), Fe(1)–S(1)–Fe(2) 98.19(5), Fe(1)–S(2)–Fe(2) 98.05(5), Fe(1)–C(5)–O(5) 130.5(4), Fe(1)–C(5)–C(7) 112.9(3), Fe(2)–C(6)–C(13) 111.0(3), Fe(2)–C(6)–O(6) 131.9(4), C(6)–C(13)–N(3) 108.6(4), C(5)–C(7)–N(2) 110.4(4)°.

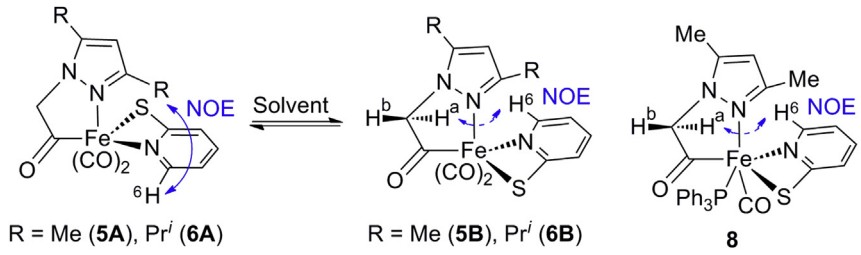

Scheme 2. The isomerization of complexes **5** and **6** as well as the NOE of complexes **5**, **6** and **8**.

H^6 of pyridyl, indicating the proximity of the 3-methyl of pyrazolyl to the pyridyl ring. This spatial arrangement fitted the three-dimensional description of the isomer with the pyridyl ring *trans* to the bridging acyl and thus assigned the signal set with larger integrals to **5A**. The NOE signals were attenuated for **5B** due to the relatively small amount of the isomer but still recognizable. A correlation between the methylene proton at 4.39 ppm and the aromatic proton at 7.51 ppm was consistent with the structure of **5B**, corroborating the above NMR assignment of **5A** and differentiated the methylene proton H^a with H^b as well, since only one of the methylene protons could spatially approach the pyridyl ring. The structural difference of isomers **A** and **B** mainly originates from the relative location between 2-pyridinethiolate and (pyrazol-1-yl) acyl. It is also interesting that the relative ratio of isomers **5A** and **5B** is different in the $CDCl_3$ and acetone-d_6 solutions, reflecting that the conversion between isomer **A** and isomer **B** is possible in solution. Moreover, this conversion can be explained by a plausible pathway through the partial dissociation of the nitrogen ligands and succedent association process with the help of solvent [33,34].

The structure of isomer **5A** has been confirmed by X-ray crystal structural analyses, and is presented in Fig. 2, which shows the pyridyl nitrogen atom occupies the position *trans* to the acyl group with the angle C(3)–Fe(1)–N(1) of 160.51(9)°. The shortest distance between H^6 of pyridyl and 3-methyl protons of pyrazolyl is 2.771 Å, suggesting the NOE correlation between these protons as shown by the NOE experiments. Other structural parameters such as Fe–N, Fe–S and Fe–C_{acyl} bond distances are analogous to those in **3**.

2.3. Reaction of (pyrazol-1-yl)acyl iron complexes with PPh_3

Treatment of **3** with PPh_3 at room temperature rendered the decomposition of the starting material, which was significantly different from the reactivity of the related thiolate diiron derivatives with the μ-SR groups [19,35,36]. The reason for this dissimilarity is not completely clear at present, which may be attributed to the instability of the resulting products as well as the easy reductive elimination from **3**. Although the decomposition reaction occurred upon treatment of **3** with PPh_3, complexes **7**–**9** were successfully obtained by the substitution of carbonyl in **1**, **5** and **6** by PPh_3, and characterized by IR and NMR spectroscopy. Their acyl carbonyl absorption frequencies (1641–1655 cm^{-1}) were close to those of **5** and **6**. Their ^1H, ^{13}C and ^{31}P NMR showed only one set of proton, carbon and phosphorous signals, which unanimously confirmed that these three complexes had no isomers in solution, unlike complexes **5** and **6**. Moreover, like that in **5B**, the obvious NOE correlation between H^6 of pyridyl and one methylene proton H^a was also observed in **8** (Scheme 2), suggesting that 2-pyridinethiolate and (pyrazol-1-yl)acyl should be in the same relative location in these two complexes. A computational modeling suggested that **8** is more stable by 3.0 kcal/mol than its potential isomer that has a structure analogous to **5A**, explaining the exclusive existence of **8**, while in the case of **5** the two isomers have an energy difference of only 0.2 kcal/mol (see the Supplementary materials). This clear energy difference in the case of **8** most probably comes from the preference of aligning the electronegative ligands, namely the triphenylphosphine and the pyridyl ring, in *trans* positions. While two same carbonyl ligands in **5** minimized this effect and radically reduced the energy difference.

The structures of **7**–**9** were confirmed by X-ray crystallography, and are shown in Figs. 3–5, respectively. Fig. 3 shows that the iron atom adopts a six-coordinate distorted octahedral geometry with the iodine and phosphorous atoms in a *trans* configuration. The

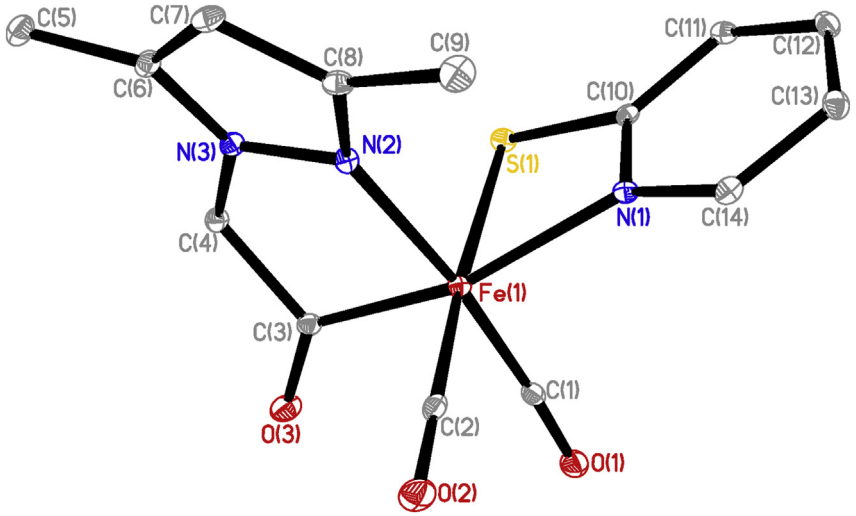

Fig. 2. The molecular structure of **5A**. The thermal ellipsoids are drawn at the 30% probability level. Selected bond distances (Å) and angles (°): Fe(1)–S(1) 2.3764(7), Fe(1)–N(1) 2.053(2), Fe(1)–N(2) 1.989(2), Fe(1)–C(3) 1.935(3), C(3)–O(3) 1.214(3), C(3)–C(4) 1.538(3) Å; N(1)–Fe(1)–S(1) 69.82(6), C(3)–Fe(1)–N(2) 82.9(1), C(1)–Fe(1)–N(2) 172.3(1), N(2)–Fe(1)–S(1) 90.62(6), C(3)–Fe(1)–N(1) 160.51(9), Fe(1)–C(3)–O(3) 130.7(2), Fe(1)–C(3)–C(4) 111.5(2), Fe(1)–S(1)–C(10) 78.91(8), C(3)–C(4)–N(3) 108.5(2)°.

angle P(1)–Fe(1)–I(1) is 170.34(2)°. Figs. 4 and 5 show that the fundamental frameworks in complexes **8** and **9** are similar to each other. In these two complexes, the sulfur atom instead of the pyridyl nitrogen occupies the position *trans* to the acyl group with the angle C(2)–Fe(1)–S(1) of 161.9(1)° for **8** and 160.91(7)° for **9**, respectively. The shortest distance between H^6 of pyridyl and the methylene protons is 2.737 Å, in the range of the NOE correlation between these protons. The structural features of **8** and **9** also indirectly support the suggested structures of isomers **5B** and **6B**, since the resembling NOE between H^6 of pyridyl and one of the methylene protons was observed in **5B** and **8**. Complexes **7**–**9** possess analogous Fe–N, Fe–C_{acyl} and C–C_{acyl} bond distances, which are also comparable to those in **1** and **5A**, as well as the corresponding values in some model complexes for the active site of [Fe]-hydrogenase [16–20].

In summary, (pyrazol-1-yl)acyl iron complexes are readily obtained through the reaction of 1-lithio derivatives of 1-methyl-3,5-dialkylpyrazoles with $Fe(CO)_5$ followed by I_2, which can be good starting materials for new acyl iron species with interesting structural features because of their high chemical reactivity. Although several kinds of mimics of the [Fe]-hydrogenase active site bearing acyl [20], acylphosphine [16], carbamoylpyridine [18] and acylmethylpyridine [21,25] ligands have appeared in literature, other structural models should be welcome to gain deeply understanding of the structure and catalytic function of [Fe]-hydrogenase. These newly synthesized acylmethylpyrazole iron complexes may be used as potential models for the active site of [Fe]-hydrogenase, which is in progress.

3. Experimental

All reactions were carried out under an atmosphere of argon. Solvents were dried and freshly distilled prior to use according to standard procedures. NMR spectra were recorded on a Bruker 400 spectrometer using $CDCl_3$ as solvent unless otherwise noted, and the chemical shifts were reported in ppm with respect to the reference (internal $SiMe_4$ for ^1H and ^{13}C NMR spectra, external 85% H_3PO_4 aqueous solution for ^{31}P NMR spectra). IR spectra were recorded as KBr pellets on a Nicolet 380 spectrometer. Elemental analyses were carried out on an Elementar Vairo EL analyzer. HR mass spectra were obtained on a Varian QFT-ESI spectrometer. Melting points were measured with an X-4 digital micro melting-point apparatus and were uncorrected.

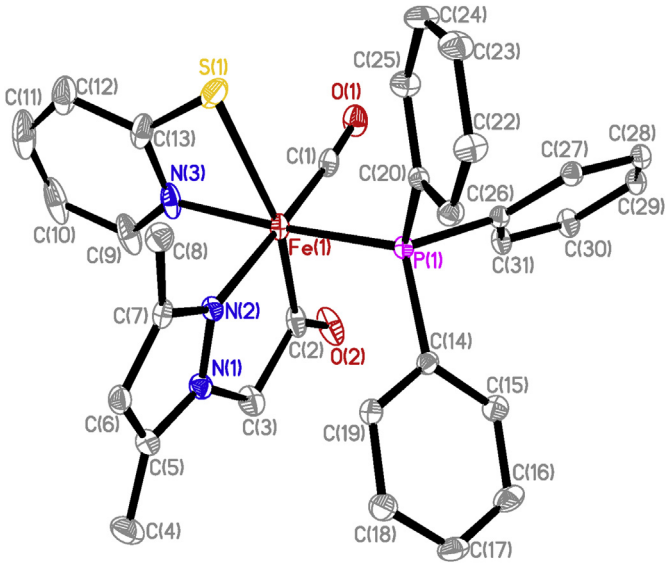

Fig. 4. The molecular structure of **8**. The thermal ellipsoids are drawn at the 30% probability level. Selected bond distances (Å) and angles (°): Fe(1)–P(1) 2.239(1), Fe(1)–S(1) 2.471(1), Fe(1)–N(2) 2.011(2), Fe(1)–N(3) 2.001(3), Fe(1)–C(2) 1.901(3), C(2)–O(2) 1.224(4), C(2)–C(3) 1.549(5) Å; N(3)–Fe(1)–P(1) 173.0(1), C(1)–Fe(1)–N(2) 176.0(1), N(3)–Fe(1)–S(1) 68.7(1), C(2)–Fe(1)–N(2) 84.5(1), C(2)–Fe(1)–S(1) 161.9(1), Fe(1)–S(1)–C(13) 76.5(1), Fe(1)–C(2)–O(2) 131.1(3), Fe(1)–C(2)–C(3) 113.7(2), Fe(1)–P(1)–C(26) 116.5(1), C(20)–P(1)–C(26) 100.8(1), C(2)–C(3)–N(1) 109.7(3)°.

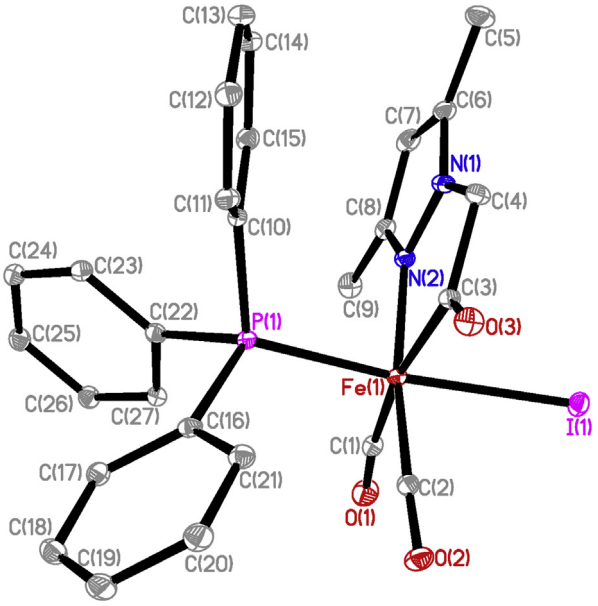

Fig. 3. The molecular structure of **7**. The thermal ellipsoids are drawn at the 30% probability level. Selected bond distances (Å) and angles (°): Fe(1)–I(1) 2.676(1), Fe(1)–C(3) 1.973(3), Fe(1)–N(2) 1.984(2), Fe(1)–P(1) 2.273(1), C3–O(3) 1.211(3), C3–C(4) 1.543(4) Å; P(1)–Fe(1)–I(1) 170.34(2), N(2)–Fe(1)–C(3) 83.5(1), Fe(1)–C(3)–O(3) 129.9(2), Fe(1)–C(3)–C(4) 112.8(2), Fe(1)–P(1)–C(22) 119.93(9), C(10)–P(1)–C(22) 101.8(2), C(3)–C(4)–N(1) 110.1(2)°.

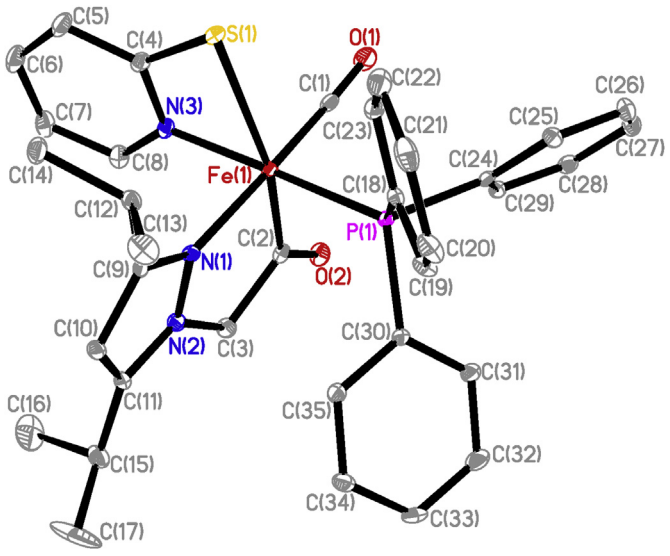

Fig. 5. The molecular structure of **9**. The thermal ellipsoids are drawn at the 30% probability level. Selected bond distances (Å) and angles (°): Fe(1)–P(1) 2.2620(7), Fe(1)–S(1) 2.4935(7), Fe(1)–N(1) 2.024(2), Fe(1)–N(3) 2.007(2), Fe(1)–C(2) 1.894(2), C(2)–O(2) 1.232(3), C(2)–C(3) 1.539(3) Å; N(3)–Fe(1)–P(1) 174.04(6), C(1)–Fe(1)–N(1) 175.6(1), N(3)–Fe(1)–S(1) 68.33(6), C(2)–Fe(1)–N(1) 84.74(9), C(2)–Fe(1)–S(1) 160.91(7), Fe(1)–C(2)–O(2) 130.9(2), Fe(1)–C(2)–C(3) 114.1(2), Fe(1)–P(1)–C(18) 116.92(8), C(18)–P(1)–C(30) 101.8(1), C(13)–C(12)–C(14) 111.1(2), C(16)–C(15)–C(17) 113.1(3), C(2)–C(3)–N(2) 110.4(2)°.

3.1. Synthesis of 1,3,5-trimethylpyrazole and 1-methyl-3,5-diisopropylpyrazole

NaH (60 mmol) was added to the solution of 3,5-dimethylpyrazole or 3,5-diisopropylpyrazole (50 mmol) in THF (40 ml) at room temperature. The resulting mixture was stirred for 1 h, and then CH_3I (50 mmol) was added. After the reaction mixture was continuously stirred overnight at room temperature, water (100 ml) was added slowly. The solution was extracted with ethyl acetate (3 × 50 ml). The organic layers were combined, washed with saturated brine and dried over anhydrous $MgSO_4$. The solvent was removed *in vacuo* to give the expected products.

1,3,5-Trimethylpyrazole, yield: 46%. ^{1}H NMR: δ 2.18 (s, 3H), 2.19 (s, 3H) (CH_3), 3.67 (s, 3H, NCH_3), 5.76 (s, 1H, H^4 of pyrazole) ppm. ^{13}C NMR: δ 11.0, 13.4 (CH_3), 35.6 (NCH_3), 104.8 (C^4 of pyrazole), 139.0, 147.0 (C^3 and C^5 of pyrazole) ppm.

1-Methyl-3,5-diisopropylpyrazole, yield: 43%. ^{1}H NMR: δ 1.23 (d, J = 1.8 Hz, 6H), 1.25 (d, J = 1.9 Hz, 6H) (CH_3), 2.85–2.95 (m, 2H, CH), 3.75 (s, 3H, NCH_3), 5.82 (s, 1H, H^4 of pyrazole) ppm. ^{13}C NMR: δ 22.3, 23.0 (CH_3), 25.5, 27.9 (CH), 35.7 (NCH_3), 98.1 (C^4 of pyrazole), 149.6, 157.8 (C^3 and C^5 of pyrazole) ppm.

3.2. Synthesis of $CH_2(CO)$ (3,5-Me_2Pz)Fe$(CO)_3$I (**1**)

A hexane solution of *n*-BuLi (1.6 M, 0.63 ml, 1 mmol) was added to the solution of 1,3,5-trimethylpyrazole (0.11 g, 1 mmol) in THF (30 ml) at −78 °C. The resulting mixture was stirred for 1 h at that temperature, and then $Fe(CO)_5$ (0.13 ml, 1 mmol) was added. The reaction mixture was continuously stirred at −78 °C for 0.5 h, allowed to reach room temperature slowly and stirred for 2 h. Then, a solution of I_2 (0.25 g, 1 mmol) in THF (10 ml) was added dropwise. After completion of addition, the reaction mixture was stirred overnight. The solvent was removed under reduced pressure, and the residue was purified by column chromatography on silica with CH_2Cl_2 as the eluent. The red eluate was concentrated to dryness to give **1** as a red solid. Yield: 0.12 g (30%), mp 43–50 °C (dec.). ^{1}H NMR: δ 2.36 (s, 3H), 2.49 (s, 3H) (CH_3), 4.52 (d, J = 16.2 Hz, 1H), 5.08 (d, J = 16.2 Hz, 1H) (CH_2), 6.10 (s, 1H, H^4 of pyrazole) ppm. ^{13}C NMR: δ 12.5, 15.6 (CH_3), 67.2 (CH_2), 109.9 (C^4 of pyrazole), 141.7, 152.1 (C^3 and C^5 of pyrazole), 200.5, 206.7, 207.5 (C≡O), 254.0 (C═O) ppm. IR: $\nu_{C\equiv O}$ = 2087 (vs), 2041 (vs), 2014 (vs), 1979 (sh); $\nu_{C=O}$ = 1667 (s) cm^{-1}. Anal. Calc. for $C_{10}H_9FeIN_2O_4$: C, 29.73; H, 2.25; N, 6.94. Found: C, 29.47; H, 2.50; N, 6.73%.

3.3. Synthesis of $CH_2(CO)$ (3,5-Pr^i_2Pz)Fe$(CO)_3$I (**2**)

This complex was similarly obtained as above-mentioned for **1**, while 1,3,5-trimethylpyrazole was replaced by 1-methyl-3,5-diisopropylpyrazole. Yield: 26%, mp 41–44 °C (dec.). ^{1}H NMR: δ 1.30 (d, J = 3.8 Hz, 3H), 1.32 (d, J = 3.8 Hz, 3H), 1.38 (d, J = 6.8 Hz, 3H), 1.43 (d, J = 6.8 Hz, 3H) (CH_3), 2.88–2.98 (m, 1H), 3.18–3.29 (m, 1H) (CH), 4.58 (d, J = 16.1 Hz, 1H), 5.17 (d, J = 16.1 Hz, 1H) (CH_2), 6.15 (s, 1H, H^4 of pyrazole) ppm. ^{13}C NMR: δ 21.5, 21.8, 22.9 (2 × C) (CH_3), 27.1, 29.4 (CH), 66.6 (CH_2), 102.6 (C^4 of pyrazole), 152.6, 162.4 (C^3 and C^5 of pyrazole), 200.6, 207.0, 207.6 (C≡O), 254.2 (C═O) ppm. IR: $\nu_{C\equiv O}$ = 2087 (vs), 2047 (vs), 2008 (vs), 1975 (sh); $\nu_{C=O}$ = 1676 (s) cm^{-1}. Anal. Calc. for $C_{14}H_{17}FeIN_2O_4$: C, 36.55; H, 3.72; N, 6.09. Found: C, 36.72; H, 3.53; N, 6.35%.

3.4. Synthesis of $[CH_2(CO)$ (3,5-Me_2Pz)Fe$(CO)_2$(SPh)$]_2$ (**3**)

NaH (9.1 mg, 0.38 mmol) was added to a solution of PhSH (39.5 μl, 0.38 mmol) in CH_2Cl_2 (15 ml). The reaction mixture was stirred for 2 h at room temperature, followed by the addition of a solution of **1** (154 mg, 0.38 mmol) in CH_2Cl_2 (10 ml). The resulting mixture was continuously stirred for 6 h. The solvent was removed under reduced pressure, and the residue was purified by column chromatography on silica with ethyl acetate/hexane (1:1, v/v) as the eluent. The yellow eluate was concentrated to dryness to afford 90 mg (66%) of **3**. Mp 66–70 °C (dec.). ^{1}H NMR: δ 2.30 (s, 6H), 2.31 (s, 6H) (CH_3), 3.92 (d, J = 15.4 Hz, 2H), 4.48 (d, J = 15.4 Hz, 2H) (CH_2), 6.04 (s, 2H, H^4 of pyrazole), 7.15 (t, J = 7.3 Hz, 2H), 7.25 (t, J = 7.9 Hz, 4H), 7.68 (d, J = 7.7 Hz, 4H) (C_6H_5) ppm. ^{13}C NMR: δ 12.2, 15.5 (CH_3), 64.4 (CH_2), 109.1 (C^4 of pyrazole), 125.5, 128.8, 131.4, 138.6 (C_6H_5), 140.6, 154.2 (C^3 and C^5 of pyrazole), 207.1, 213.4 (C≡O), 262.2 (C═O) ppm. IR: $\nu_{C\equiv O}$ = 2087 (vs), 2037 (vs, br), 1977 (vs); $\nu_{C=O}$ = 1678 (s) cm^{-1}. Anal. Calc. for $C_{30}H_{28}Fe_2N_4O_6S_2$: C, 50.30; H, 3.94; N, 7.82. Found: C, 50.12; H, 3.63; N, 7.95%.

3.5. Reaction of **3** with PPh_3

PPh_3 (51 mg, 0.19 mmol) was added to the solution of **3** (70 mg, 0.098 mmol) in CH_2Cl_2 (15 ml), the resulting reaction mixture was stirred overnight at room temperature. After the solvent was removed under reduced pressure, the residue was separated by column chromatography on silica. This reaction yielded no characterizable products.

3.6. Thermal decomposition reaction of **3**

The solution of **3** (86 mg, 0.12 mmol) in toluene (10 ml) was stirred and heated at 45 °C for 6 h. The solvent was removed under reduced pressure, and the residue was purified by column chromatography on silica with ethyl acetate as the eluent. The eluate was concentrated to dryness to give compound **4** as a slightly yellow liquid. Yield: 18 mg (31%). ^{1}H NMR: δ 2.21 (s, 6H, CH_3), 4.88 (s, 2H, CH_2), 5.87 (s, 1H, H^4 of pyrazole), 7.32–7.35 (m, 5H, C_6H_5) ppm. ^{13}C NMR: δ 11.2, 13.6 (CH_3), 57.6 (CH_2), 106.5 (C^4 of pyrazole), 126.2, 129.3, 129.7, 134.6 (C_6H_5), 140.7, 149.3 (C^3 and C^5 of pyrazole), 195.0 (C═O) ppm. HRMS–ESI (m/z): 269.0722 (Calc. for $C_{13}H_{14}N_2NaOS$: 269.0725, $[M+Na]^+$, 100%).

When the toluene solution of **3** was stirred and heated at reflux for 3 h, PhSSPh was obtained in 52% yield after column chromatography on silica with hexane as the eluent, and confirmed by comparison of NMR spectroscopic data with those of the authentic sample of PhSSPh. In addition, PhSSPh was obtained in *ca.* 25% yield with other uncharacterizable products when heating **4** in refluxing toluene.

3.7. Synthesis of $CH_2(CO)$ (3,5-Me_2Pz)Fe$(CO)_2$(SPy) (**5**)

This complex was similarly obtained as above-mentioned for **3**, but PhSH was replaced by 2-mercaptopyridine. Yield: 57%, mp 70–77 °C (dec.). Complex **5** displayed two isomers (**5A**/**5B**) in solution. The relative ratio of isomers **5A**/**5B** was *ca.* 4/1 in $CDCl_3$ and 3/1 in acetone-d_6, respectively, according to the integration of the corresponding protons of the methylene group. ^{1}H NMR of isomer of **5A**: δ 1.68 (s, 3-CH_3 of pyrazole), 2.30 (s, 5-CH_3 of pyrazole), 4.24 (d, J = 15.8 Hz), 4.51 (d, J = 15.8 Hz) (CH_2), 5.94 (s, H^4 of pyrazole), 6.67 (d, J = 8.1 Hz, H^3 of pyridyl), 6.81 (t, J = 6.0 Hz, H^5 of pyridyl), 7.36 (t, J = 7.5 Hz, H^4 of pyridyl), 8.10 (d, J = 4.6 Hz, H^6 of pyridyl) ppm. ^{1}H NMR of isomer of **5B**: δ 2.30 (s, 5-CH_3 of pyrazole), 2.62 (s, 3-CH_3 of pyrazole), 4.30 (d, J = 16.7 Hz, H^b of CH_2), 4.39 (d, J = 16.7 Hz, H^a of CH_2), 5.96 (s, H^4 of pyrazole), 6.66 (t, J = 5.8 Hz, H^5 of pyridyl), 7.51 (d, J = 4.5 Hz, H^6 of pyridyl), 7.26 (t, J = 7.4 Hz, H^4 of pyridyl), 7.63 (s, br, H^3 of pyridyl) ppm. These assignments were confirmed by standard Bruker gradient enhanced NOE pulse sequences. ^{1}H NMR of isomer of **5A** (acetone-d_6): δ 1.70 (s, 3-CH_3 of pyrazole), 2.37 (s, 5-CH_3 of pyrazole), 4.39 (d, J = 16.1 Hz), 4.53 (d, J = 16.1 Hz) (CH_2), 6.08 (s, H^4 of pyrazole), 6.77 (d, J = 8.3 Hz, H^3 of

pyridyl), 6.95–6.99 (m, H^5 of pyridyl), 7.51 (t, J = 8.0 Hz, H^4 of pyridyl), 8.35 (d, J = 4.8 Hz, H^6 of pyridyl) ppm. ^{1}H NMR of isomer of **5B** (acetone-d_6): δ 2.33 (s, 5-CH_3 of pyrazole), 2.61 (s, 3-CH_3 of pyrazole), 4.51 (d, J = 16.8 Hz), 4.76 (d, J = 16.8 Hz) (CH_2), 6.09 (s, H^4 of pyrazole), 7.40 (t, J = 8.0 Hz), 7.72 (d, J = 5.8 Hz) (protons of pyridyl) ppm. The other two protons of the pyridyl group overlapped with those of the pyridyl group of isomer **5A**. ^{13}C NMR of isomer of **5A** (acetone-d_6): δ 12.1, 13.5 (CH_3), 64.9 (CH_2), 109.0 (C^4 of pyrazole), 117.2, 125.7, 135.6, 150.4, 178.0 (carbons of pyridyl), 140.0, 151.7 (C^3 and C^5 of pyrazole), 208.6, 211.7 (C≡O), 265.2 (C═O) ppm. ^{13}C NMR of isomer of **5B** (acetone-d_6): δ 12.2, 15.9 (CH_3), 64.8 (CH_2), 109.3 (C^4 of pyrazole), 116.8, 127.0, 135.7, 148.0, 181.3 (carbons of pyridyl), 140.5, 154.2 (C^3 and C^5 of pyrazole), 210.2, 211.1 (C≡O), 269.1 (C═O) ppm. IR: $\nu_{C\equiv O}$ = 2030 (vs), 1967 (vs); $\nu_{C=O}$ = 1650 (s) cm^{-1}. Anal. Calc. for $C_{14}H_{13}FeN_3O_3S$: C, 46.81; H, 3.65; N, 11.70. Found: C, 46.58; H, 3.74; N, 11.94%.

3.8. Synthesis of $CH_2(CO)$ (3,5-Pr^i_2Pz)$Fe(CO)_2$(SPy) (**6**)

This complex was similarly obtained by the reaction of **2** with 2-mercaptopyridine as above-mentioned reaction of **1** with PhSH. Yield: 53%, mp 66–76 °C (dec.). Complex **6** also displayed two isomers (**6A**/**6B**) in $CDCl_3$ solution. The relative ratio of isomers **6A**/**6B** was *ca.* 3/1 according to the integration of the corresponding protons of one methyl group. ^{1}H NMR of isomer of **6A**: δ 0.54 (d, J = 6.8 Hz, CH_3), 1.19 (d, J = 6.9 Hz, CH_3), 1.21–1.30 (m, CH_3 of **6A**/**6B**), 2.47–2.57 (m, C*H*), 2.82–2.92 (m, C*H*), 4.27 (d, J = 15.6 Hz), 4.57 (d, J = 15.6 Hz) (CH_2), 6.01 (s, H^4 of pyrazole), 6.75 (d, J = 8.2 Hz), 6.84–6.87 (m), 7.33 (dt, J = 1.6 and 8.3 Hz), 8.11 (d, J = 5.1 Hz) (protons of pyridyl) ppm. ^{1}H NMR of isomer of **6B**: δ 1.09 (d, J = 6.8 Hz, CH_3), 4.34 (d, J = 16.6 Hz), 4.42 (d, J = 16.6 Hz) (CH_2), 6.03 (s, H^4 of pyrazole), 6.62–6.66 (m), 6.81–6.83 (m), 7.50 (d, J = 5.3 Hz), 8.47 (d, J = 4.7 Hz) (protons of pyridyl) ppm. The methine proton and part of methyl proton signals overlapped each other in isomers **6A**/**6B**. ^{13}C NMR of isomer **6A**: δ 21.5, 21.8, 22.5, 23.3 (CH_3), 26.8, 27.3 (C*H*), 64.6 (CH_2), 101.2 (C^4 of pyrazole), 117.6, 125.8, 135.4, 150.9, 177.9 (carbons of pyridyl), 147.9, 151.1 (C^3 and C^5 of pyrazole), 208.8, 211.7 (C≡O), 265.1 (C═O) ppm. ^{13}C NMR of isomer **6B**: δ 21.4, 21.9, 23.5, 23.6 (CH_3), 26.8, 27.4 (C*H*), 64.4 (CH_2), 102.0 (C^4 of pyrazole), 116.8, 127.1, 135.7, 149.6, 181.2 (carbons of pyridyl), 137.4, 151.5 (C^3 and C^5 of pyrazole), 210.2, 211.2 (C≡O) ppm. The acyl carbon signal (C═O) was not observed owing to the relatively low contents of isomer **6B** and low sensitivity of the carbonyl carbon. IR: $\nu_{C\equiv O}$ = 2031 (vs), 1968 (vs); $\nu_{C=O}$ = 1655 (s) cm^{-1}. Anal. Calc. for $C_{18}H_{21}FeN_3O_3S$: C, 52.06; H, 5.10; N, 10.12. Found: C,52.36; H, 4.87; N, 10.45%.

3.9. Synthesis of $CH_2(CO)$ (3,5-Me_2Pz)$Fe(CO)_2(PPh_3)$I (**7**)

PPh_3 (97 mg, 0.37 mmol) was added to a solution of **1** (0.15 g, 0.37 mmol) in CH_2Cl_2 (15 ml). The resulting mixture was stirred overnight at room temperature. The solvent was removed under reduced pressure, and the residue was purified by column chromatography on silica with hexane as the eluent firstly to remove the starting materials, then with CH_2Cl_2 as the eluent to give a red eluate, which was concentrated to dryness to afford 80 mg (34%) of **7** as a red solid. Mp 56–58 °C. ^{1}H NMR: δ 2.09 (s, 6H, CH_3), 2.98 (d, J = 16.1 Hz, 1H), 4.53 (d, J = 16.1 Hz, 1H) (CH_2), 6.01 (s, 1H, H^4 of pyrazole), 7.21–7.23 (m, 6H), 7.33–7.37 (m, 6H), 7.44–7.47 (m, 3H) (C$_6H_5$). ^{13}C NMR: δ 12.5, 15.2 (CH_3), 66.1 (d, $J_{P\text{-}C}$ = 2.0 Hz, CH_2), 109.7 (C^4 of pyrazole), 128.5 (d, $J_{P\text{-}C}$ = 9.8 Hz), 130.7 (d, $J_{P\text{-}C}$ = 2.0 Hz), 131.8 (d, $J_{P\text{-}C}$ = 42.3 Hz), 133.4 (d, $J_{P\text{-}C}$ = 9.6 Hz) (C$_6H_5$), 140.6, 151.9 (C^3 and C^5 of pyrazole), 210.7 (d, $J_{P\text{-}C}$ = 8.7 Hz), 215.4 (d, $J_{P\text{-}C}$ = 25 Hz) (C≡O), 275.4 (d, $J_{P\text{-}C}$ = 25.2 Hz, C═O). ^{31}P NMR: δ 61.8. IR (cm^{-1}): $\nu_{C\equiv O}$ = 2016 (vs), 1969 (vs); $\nu_{C=O}$ = 1641 (s). Anal. Calc. for $C_{27}H_{24}FeIN_2O_3P$: C, 50.81; H, 3.79; N, 4.39. Found: C, 50.98; H, 3.92; N, 4.17%.

3.10. Synthesis of $CH_2(CO)$ (3,5-Me_2Pz)$Fe(CO)$ (PPh_3) (SPy) (**8**)

This complex was similarly obtained as above-mentioned for **7**, while **1** was replaced by **5**. After the solvent was removed under reduced pressure, the residue was purified by column chromatography on silica with ethyl acetate/hexane (1:3, v/v) as the eluent firstly to remove the starting materials, then with ethyl acetate/hexane (1:1, v/v) as the eluent to give a yellow eluate, which was concentrated to dryness to afford 20 mg (31%) of **8** as a yellow solid. Mp 50–66 °C (dec.). ^{1}H NMR: δ 1.99 (s, 3H), 2.20 (s, 3H) (CH_3), 3.01 (d, J = 16.3 Hz, 1H), 3.94 (d, J = 16.3 Hz, 1H) (CH_2), 5.81 (s, 1H, H^4 of pyrazole), 6.48 (t, J = 6.3 Hz, 1H), 6.71 (d, J = 8.2 Hz, 1H), 7.09–7.14 (m, 1H), 7.28–7.39 (m, 16H) (C$_5H_4$N and C$_6H_5$) ppm. The obvious NOE correlations between the methylene protons and the pyridyl as well as phenyl protons were observed, although these two methylene protons were barely distinguishable owing to the serious overlap among the signals of the pyridyl and phenyl protons. ^{13}C NMR: δ 12.0, 15.6 (CH_3), 64.2 (d, $J_{P\text{-}C}$ = 5.6 Hz, CH_2), 109.4 (C^4 of pyrazole), 116.2, 125.6 (d, $J_{P\text{-}C}$ = 3.6 Hz), 128.0 (d, $J_{P\text{-}C}$ = 9.4 Hz), 129.7 (d, $J_{P\text{-}C}$ = 2.1 Hz), 132.9, 133.5 (d, $J_{P\text{-}C}$ = 9.8 Hz), 134.5, 139.3, 148.9, 153.6, 179.5 (C$_6H_5$, C$_5H_4$N as well as C^3 and C^5 of pyrazole) ppm. The carbonyl carbon signals were not observed possibly owing to low solubility and low sensitivity of carbonyl carbon. ^{31}P NMR: δ 56.6 ppm. IR: $\nu_{C\equiv O}$ = 1952 (vs); $\nu_{C=O}$ = 1648 (s) cm^{-1}. Anal. Calc. for $C_{31}H_{28}FeN_3O_2PS$: C, 62.74; H, 4.76; N, 7.08. Found: C, 62.94; H, 4.51; N, 7.23%.

3.11. Synthesis of $CH_2(CO)$ (3,5-Pr^i_2Pz)$Fe(CO)$ (PPh_3) (SPy) (**9**)

This complex was similarly obtained as above-mentioned for **7**, while **1** was replaced by **6**. The workup was carried out according to the synthesis of **8**. Yield: 32%, mp 52–61 °C (dec.). ^{1}H NMR: δ 0.71 (d, J = 6.9 Hz, 3H, CH_3), 0.88 (d, J = 6.7 Hz, 3H, CH_3), 1.12 (d, J = 6.8 Hz, 3H, CH_3), 1.18 (d, J = 6.9 Hz, 3H, CH_3), 2.54–2.61 (m, 1H, C*H*), 3.09 (d, J = 16.3 Hz, 1H, CH_2), 4.00–4.06 (m, 2H, CH_2 and C*H*), 5.96 (s, 1H, H^4 of pyrazole), 6.47 (t, J = 6.3 Hz, 1H), 6.73 (d, J = 8.1 Hz, 1H), 7.12 (t, J = 7.6 Hz, 1H) (C$_5H_4$N), 7.28–7.41 (m, 16H, C$_5H_4$N and C$_6H_5$) ppm. ^{13}C NMR: δ 21.6, 21.7, 22.5, 25.4 (CH_3), 26.5, 27.6 (C*H*), 63.8 (d, $J_{P\text{-}C}$ = 4.3 Hz, CH_2), 101.9 (C^4 of pyrazole), 116.1, 125.8, 128.0 (d, $J_{P\text{-}C}$ = 9.1 Hz), 128.5 (d, $J_{P\text{-}C}$ = 11.6 Hz), 129.7, 132.1 (d, $J_{P\text{-}C}$ = 9.8 Hz), 133.5 (d, $J_{P\text{-}C}$ = 9.7 Hz), 134.4, 148.6, 150.8, 180.0 (C$_6H_5$, C$_5H_4$N as well as C^3 and C^5 of pyrazole), 218.4 (d, $J_{P\text{-}C}$ = 30.0 Hz, C≡O), 291.7 (d, $J_{P\text{-}C}$ = 22.6 Hz, C═O) ppm. ^{31}P NMR: δ 54.9 ppm. IR: $\nu_{C\equiv O}$ = 1957 (vs); $\nu_{C=O}$ = 1655 (s) cm^{-1}. Anal. Calc. for $C_{35}H_{36}FeN_3O_2PS$: C, 64.72; H, 5.59; N, 6.47. Found: C, 64.56; H, 5.62; N, 6.74%.

3.12. Crystal structure determinations

Crystals of **3**, **5A** and **7**–**9** suitable for X-ray analyses were obtained by slow diffusion of hexane into their CH_2Cl_2 solutions at −18 °C. All intensity data were collected on a SuperNova Eos detector for **3**, **5A** and **9** as well as Rigaku Saturn CCD detector for **7** and **8** using graphite monochromated Mo-Kα radiation (λ = 0.71073 Å). Semi-empirical absorption corrections were applied using the Crystalclear program [37]. The structures were solved by direct methods and difference Fourier map using SHELXS of the SHELXTL package and refined with SHELXL [38] by full-matrix least-squares on F^2. All non-hydrogen atoms were refined anisotropically. Hydrogen atoms were added geometrically and refined with riding model position parameters. A summary of the fundamental crystal data for **3**, **5A** and **7**–**9** is listed in Table 1.

Table 1
Crystal data and refinement parameters for complexes **3**, **5A** and **7**–**9**.

Complex	**3**	**5A**	**7**	**8**	**9**
Formula	$C_{30}H_{28}Fe_2N_4O_6S_2$	$C_{14}H_{13}FeN_3O_3S$	$C_{27}H_{24}FeIN_2O_3P$	$C_{31}H_{28}FeN_3O_2PS$	$C_{35}H_{36}FeN_3O_2PS$
Formula weight	716.38	355.20	638.20	593.44	649.55
Crystal size (mm)	0.04 × 0.02 × 0.01	0.30 × 0.30 × 0.20	0.20 × 0.18 × 0.12	0.20 × 0.18 × 0.10	0.50 × 0.30 × 0.15
Crystal system	Monoclinic	Monoclinic	Triclinic	Monoclinic	Monoclinic
Space group	$P2_1/c$	$C2/c$	$P\bar{1}$	$P2_1/n$	$P2_1/n$
a (Å)	10.5881(4)	23.776(2	8.923(4)	9.615(3)	10.6604(3)
b (Å)	19.3808(9)	8.3422(7)	9.026(4)	21.278(6)	21.8759(9)
C (Å)	17.9126(9)	15.7464(13)	16.059(7)	13.632(4)	13.8367(5)
α (°)	90	90	78.759(17)	90	90
β (°)	122.356(3)	100.58(1)	80.70(2)	91.292(6)	95.097(3)
γ (°)	90	90	88.36(2)	90	90
T (K)	293(2)	125(2)	113(2)	113(2)	129(2)
V (Å)^3	3105.1(2)	3070.2(5)	1251.9(10)	2788.3(14)	3214.0(2)
Z	4	8	2	4	4
D_c (g.cm^{-3})	1.532	1.554	1.693	1.414	1.342
F (000)	1472	1472	636	1232	1360
μ (mm^{-1})	1.118	1.133	1.932	0.707	0.620
θ Range (°)	2.42–25.01	2.83–26.50	1.30–27.93	1.77–27.88	2.96–25.01
No. of measured reflections	11556	6860	16131	25577	12944
No. of unique reflections (R_{int})	5471 (0.0752)	3177 (0.0390)	5955 (0.1214)	6636 (0.0487)	5656 (0.0351)
No. of observed reflections with ($I > 2\sigma(I)$)	3445	2574	5517	5608	4716
No. of parameters	401	201	318	354	392
GOF	0.959	1.043	1.063	1.160	1.056
Residuals R, Rw	0.0596, 0.0724	0.0422, 0.0804	0.0384, 0.0981	0.0601, 0.1064	0.0389, 0.0829

Acknowledgments

This work is supported by the National Natural Science Foundation of China (No. 21372124) and NFFTBS (No. J1103306).

Appendix A. Supplementary data

Supplementary data related to this article can be found at http://dx.doi.org/10.1016/j.jorganchem.2015.06.008.

References

[1] A.C. Wotal, R.D. Ribson, D.J. Weix, Stoichiometric reactions of acylnickel(II) complexes with electrophiles and the catalytic synthesis of ketones, Organometallics 33 (2014) 5874–5881.
[2] A. Maleckis, M.S. Sanford, Synthesis of fluoroalkyl palladium and nickel complexes via decarbonylation of acylmetal species, Organometallics 33 (2014) 3831–3839.
[3] B.D. Panthi, S.L. Gipson, A. Franken, Structural studies of some rhodium(III) acyl complexes containing bidentate phosphines, Inorg. Chim. Acta 425 (2015) 176–181.
[4] J.R. Hermanson, T.M. Figley, A.L. Seibert, A.R. Pinhas, The reactivity of a nucleophilic nickel acylate complex, J. Organomet. Chem. 693 (2008) 2061–2064.
[5] S.M. Dumbris, D.J. Díaz, L. McElwee-White, Preparation of hydantoins by catalytic oxidative carbonylation of α-amino amides, J. Org. Chem. 74 (2009) 8862–8865.
[6] L. Kollár, Modern Carbonylation Methods, Wiley-VCH Verlag GmbH & Co. KGaA, Weinheim, 2008.
[7] I. Omae, Transition metal-catalyzed cyclocarbonylation in organic synthesis, Coord. Chem. Rev. 255 (2011) 139–160.
[8] W. Ren, M. Yamane, Carbamoylation of aryl halides by molybdenum or tungsten carbonyl amine complexes, J. Org. Chem. 75 (2010) 3017–3020.
[9] B. Roberts, D. Liptrot, L. Alcaraz, T. Luker, M.J. Stocks, Molybdenum-mediated carbonylation of aryl halides with nucleophiles using microwave irradiation, Org. Lett. 12 (2010) 4280–4283.
[10] X. Wang, K. Cao, Y. Liu, B. Tsang, S. Liew, Migration insertion polymerization (MIP) of cyclopentadienyldicarbonyldiphenylphosphinopropyliron (FpP): A new concept for main chain metal-containing polymers (MCPs), J. Am. Chem. Soc. 135 (2013) 3399–3402.
[11] K. Cao, J. Ward, R.C. Amos, M.G. Jeong, K.T. Kim, M. Gauthier, D. Foucher, X. Wang, Organometallic macromolecules with piano stool coordination repeating units: chain configuration and stimulated solution behaviour, Chem. Commun. 50 (2014) 10062–10065.
[12] T. Hiromoto, K. Ataka, O. Pilak, S. Vogt, M.S. Stagni, W. Meyer-Klaucke, E. Warkentin, R.K. Thauer, S. Shima, U. Ermler, The crystal structure of C176A mutated [Fe]-hydrogenase suggests an acyl-iron ligation in the active site iron complex, FEBS Lett. 583 (2009) 585–590.
[13] S. Dey, P.K. Das, A. Dey, Mononuclear iron hydrogenase, Coord. Chem. Rev. 257 (2013) 42–63.
[14] M.J. Corr, J.A. Murphy, Evolution in the understanding of [Fe]-hydrogenase, Chem. Soc. Rev. 40 (2011) 2279–2292.
[15] J.A. Wright, P.J. Turrell, C.J. Pickett, The third hydrogenase: More natural organometallics, Organometallics 29 (2010) 6146–6156.
[16] A.M. Royer, T.B. Rauchfuss, D.L. Gray, Oxidative addition of thioesters to iron(0): Active-site models for hmd, nature's third hydrogenase, Organometallics 28 (2009) 3618–3620.
[17] A.M. Royer, M. Salomone-Stagni, T.B. Rauchfuss, W. Meyer-Klaucke, Iron acyl thiolato carbonyls: structural models for the active site of the [Fe]-Hydrogenase (Hmd), J. Am. Chem. Soc. 132 (2010) 16997–17003.
[18] P.J. Turrell, J.A. Wright, J.M.T. Peck, V.S. Oganesyan, C.J. Pickett, The third hydrogenase: A ferracyclic carbamoyl with close structural analogy to the active site of Hmd, Angew. Chem. Int. Ed. 49 (2010) 7508–7511.
[19] P.J. Turrell, A.D. Hill, S.K. Ibrahim, J.A. Wright, C.J. Pickett, Ferracyclic carbamoyl complexes related to the active site of [Fe]-hydrogenase, Dalton Trans. 42 (2013) 8140–8146.
[20] D. Chen, R. Scopelliti, X. Hu, Synthesis and reactivity of iron acyl complexes modeling the active site of [Fe]-Hydrogenase, J. Am. Chem. Soc. 132 (2010) 928–929.
[21] D. Chen, R. Scopelliti, X. Hu, [Fe]-Hydrogenase models featuring acylmethylpyridinyl ligands, Angew. Chem. Int. Ed. 49 (2010) 7512–7515.
[22] D. Chen, R. Scopelliti, X. Hu, Reversible protonation of a thiolate ligand in an [Fe]-Hydrogenase model complex, Angew. Chem. Int. Ed. 51 (2012) 1919–1921.
[23] B. Hu, D. Chen, X. Hu, Synthesis and reactivity of mononuclear iron models of [Fe]-hydrogenase that contain an acylmethylpyridinol ligand, Chem. Eur. J. 20 (2014) 1677–1682.
[24] L.-C. Song, G.-Y. Zhao, Z.-J. Xie, J.-W. Zhang, A novel acylmethylpyridinol ligand containing dinuclear iron complex closely related to [Fe]-Hydrogenase, Organometallics 32 (2013) 2509–2512.
[25] L.-C. Song, F.-Q. Hu, G.-Y. Zhao, J.-W. Zhang, W.-W. Zhang, Several new [Fe]-hydrogenase model complexes with a single Fe-center ligated to an acylmethyl(hydroxymethyl)pyridine or acylmethyl(hydroxy)pyridine ligand, Organometallics 33 (2014) 6614–6622.
[26] D.-W. Zhao, X.-L. Liu, X.-Y. Zhang, L.-F. Tang, Synthesis of acyl iron complexes based on bis(heteroaryl)methanes, J. Organomet. Chem. 780 (2015) 56–62.
[27] J.-P. Sun, D.-W. Zhao, H.-B. Song, L.-F. Tang, (Pyrazol-1-yl)carbonyl and ester-functionalized bis(pyrazol-1-yl)methide carbonyl tungsten complexes, Organometallics 33 (2014) 4425–4432.
[28] Y.-F. Xie, Z.-K. Wen, R.-Y. Tan, J. Hong, S.-B. Zhao, L.-F. Tang, bis(3,5-dimethylpyrazol-1-yl)acyl and bis(3,5-dimethylpyrazol-1-yl)methide carbonyl tungsten derivatives, Organometallics 27 (2008) 5684–5690.
[29] Q. Niu, H. Sun, L. Wang, Q. Hu, X. Li, Reactivity of mer-hydrido(2-mercaptobenzoyl)- tris(trimethylphosphine)cobalt(III) complex, Dalton Trans. 43 (2014) 4059–4066.
[30] M.R. Ringenberg, D.L. Gray, T.B. Rauchfuss, Oxidative addition of a

diphosphine anhydride to iron(0) and nickel(0): A sample approach to installing four ligands, Organometallics 30 (2011) 2885–2888.
[31] M.A. Garralda, R. Hernández, L. Ibarlucea, E. Pinilla, M.R. Torres, Synthesis and characterization of hydridoirida-α-diketones formed by the reaction of [{Ir(Cod)Cl}$_2$] (Cod = 1,5-cyclooctadiene) with *o*-(diphenylphosphino)benzaldehyde, Organometallics 22 (2003) 3600–3603.
[32] A.R. Katritzky, C. Jayaram, S.N. Vassilatos, Alpha-lithiation of N-alkyl groups in pyrazoles, Tetrahedron 39 (1983) 2023–2029.
[33] K. Ding, C.-H. Cheng, Y.-X. Yang, H.-B. Song, L.-F. Tang, Reactivity of bis(pyrazol-1-yl)methanes functionalized by 2-hydroxyphenyl and 2-methoxyphenyl on the methine carbon atom with W(CO)$_5$THF, J. Organomet. Chem. 696 (2011) 3662–3667.
[34] M.C. Carrión, F.A. Jalón, B.R. Manzano, A.M. Rodríguez, F. Sepúlveda, M. Maestro, (Arene)ruthenium(II) complexes containing substituted bis(pyrazolyl)methane ligands–Catalytic behaviour in transfer hydrogenation of ketones, Eur. J. Inorg. Chem. (2007) 3961–3973.
[35] D. Seyferth, G.B. Womack, C.M. Archer, J.C. Dewan, A simple route to hexacarbonyldiiron complexes containing a bridging thiolate and an organic bridging ligand by means of [(μ-RS) (μ-CO)Fe$_2$(CO)$_6$]$^-$ intermediates, Organometallics 8 (1989) 430–442.
[36] L. Maresca, F. Greggio, G. Sbrignadello, G. Bor, The anti-syn equilibria of the organothio bridged derivatives of iron carbonyl, (μ-RS)$_2$Fe$_2$(CO)$_6$, and of their monosubstitution products with some phosphines, (μ-RS)$_2$Fe$_2$(CO)$_5$(PR'$_3$), Inorg. Chim. Acta 5 (1971) 667–674.
[37] CrystalStructure 3.7.0 and Crystalclear 1.36: Crystal Structure Analysis Package, Rigaku and Rigaku/MSC, TX, 2000–2005.
[38] G.M. Sheldrick, A short history of SHELX, Acta Crystallogr. A64 (2008) 112–122.